J Solid State Electrochem (2004) 8: 706–717
DOI 10.1007/s10008-004-0535-8

ORIGINAL PAPER

Mihai Buda · Frank G. Gao · Allen J. Bard

Electrochemistry and electrogenerated chemiluminescence of a thin solid film of a hydrophobic tris(bipyridine) Ru(II) derivative in contact with an aqueous solution

Received: 13 March 2004 / Accepted: 5 April 2004 / Published online: 9 July 2004

Abstract The present study shows the electrochemistry, electrogenerated chemiluminescence and solid-state electroluminescence of $[Ru(bpy)_2(4,4'\text{-}(CH_3(CH_2)_{12}COO)\text{-}bpy)](ClO_4)_2$ as thin film deposited onto ITO. Cyclic voltammetry in aqueous solution of the Ru-LC film shows two reversible waves with peak potentials at about 1.27 V and −0.97 V. The apparent diffusion coefficient of the slowest species was found to be 4–6×10^{-10} cm^2/s, with a concentration of active sites of about 0.4–0.5 M.

Relatively strong ECL was observed during both oxidation and reduction, in both potential scans and potential step experiments. The reduced species appears to be much less stable than the oxidized one, as already known for other tris(bipyridine) Ru(II) derivatives in aqueous media.

Two-electrode solid-state devices prepared by Ga-In printing on the tops of Ru-LC films are similar to the $Ru(bpy)_3$ ones. The currents that flow through these devices are however about three orders of magnitude smaller than those for $Ru(bpy)_3$ devices as a result of their low electron and hole mobilities.

Keywords Electrochemiluminescence · Light-emitting devices · Modified electrodes

Dedicated to Zbigniew Galus on the occasion of his 70th birthday.

M. Buda
Dept. of Applied Physical Chemistry and Electrochemistry,
"Politehnica" University of Bucharest,
Calea Grivitei 132, 010737 Bucharest, Romania

F. G. Gao
Broadley-James Corporation, 19 Thomas Street, Irvine,
CA 92618, USA

A. J. Bard (✉)
Department of Chemistry and Biochemistry and Center
for Nano-and Molecular Science and Technology,
The University of Texas at Austin, Austin,
TX 78712, USA
E-mail: ajbard@mail.utexas.edu

Introduction

Solid-state organic light-emitting devices are widely studied because of their potential practical applications in affordable flat, active matrix displays. Light-emitting electrochemical cells (LECs) based on thin films (~100 nm) of salts of tris(bipyridine) ruthenium(II) $[Ru(bpy)_3^{2+}$ (bpy = 2,2′-bipyridine)] and its derivatives that have been studied recently [1, 2, 3] show good quantum efficiency and low operating voltages, but still rather modest operating lifetimes. These are part of a larger class of two-electrode solid-state devices that include electrochromic and photovoltaic cells that are fabricated from polymers or small molecules.

In typical two-electrode solid-state devices, one cannot study the electrodes separately because the active films in these devices are too thin to allow one to insert a reference electrode. An alternative approach is to study these film-covered electrodes individually by immersing them in a liquid electrolyte in which the film is totally insoluble. Such a liquid electrolyte contact allows one to study the film in a three-electrode set-up and, therefore, extract data during oxidation or reduction only. However, the oxidation/reduction processes are not the same as those in a two-electrode solid-state device. In a three-electrode system, during a redox process, counterions from an electrolyte either penetrate or leave the film to maintain electroneutrality. This ionic process is absent or different in a two-electrode device and may lead to different morphological changes. Moreover, movement of solvent into and out of the film can occur in solution. However, the ability to separately study the oxidation and reduction processes is attractive and may yield thermodynamic and kinetic information about the films and important insights into the overall device behavior. A good candidate for a three-electrode solid-state light-emitting device is $[Ru(bpy)_2(4,4'\text{-}(CH_3(CH_2)_{12}COO)bpy)](ClO_4)_2$, (Ru-LC, see Scheme 1 for structural details) which is insoluble in water. The present study shows its electrochemistry and electrogenerated chemilumines-

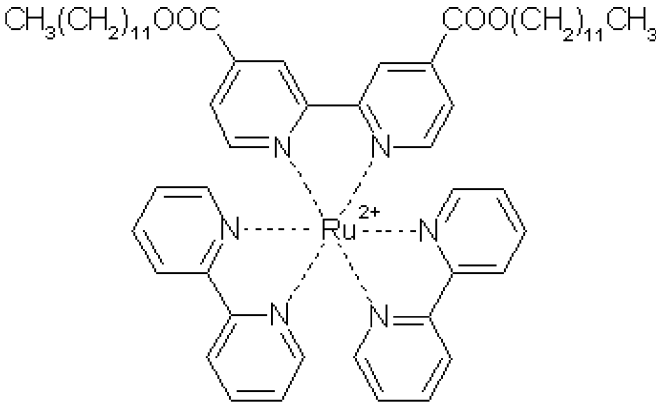

Scheme 1 Structure of $[Ru(bpy)_2(4,4'\text{-}(CH_3(CH_2)_{12}COO)bpy)]^{2+}$

cence (ECL), when it is deposited as a thin film onto conductive substrates (typically ITO).

Studies of these films are of interest in their own right as well, since they provide another example of ECL from immobilized layers, as previously observed with polymer films (such as $Ru(bpy)_3^{2+}$ in Nafion or $Ru(bpy)_3^{2+}$-containing monolayers, see [4] for a recent review).

Materials and methods

Ru-LC was prepared by a previously reported method [5]. It is totally insoluble in water, but very soluble in polar organic solvents, such as acetonitrile (MeCN) and acetone. The films were spin-coated (Headway Research) onto ITO from a 4% w/v solution in MeCN (filtered through a 0.2 μm syringe filter before spin-coating) at 2000 rpm and dried under vacuum at 60 °C for ~12 h.

Indium tin oxide (ITO)-coated glass (~20 Ω/W Delta Technologies) was thoroughly cleaned before device preparation by sonication for 20 min in a 20%(vol) solution of ethanolamine in highly pure Millipore water at ~60 °C, followed by three rinsing/sonication steps with pure water at room temperature to remove traces of ethanolamine, and drying under vacuum for several hours at ~80 °C [1].

Cyclic voltammetry was performed in aqueous solution using either 0.1 M $KClO_4$ or 0.075 M tetramethylammonium perchlorate ($TMAClO_4$) as supporting electrolyte, using an AUTOLAB electrochemical station. All experiments were performed in a sealed, three-electrode cell with a Pt wire as counter electrode and a Ag/AgCl reference; the surface area of the working electrode was ~1 cm^2. The solution was purged with Ar for ~20–30 min before each set of experiments, after which the cell was tightly sealed. Absorption spectra were taken with a Milton-Roy spectrophotometer; AFM measurements were performed with a Digital Instruments Nanoscope.

The light-emitting devices were obtained by printing a drop of Ga-In eutectic liquid alloy (Alfa-Aesar) with a syringe on top of the spin-coated film. Current-voltage and light-voltage curves for these devices were taken using an AUTOLAB electrochemical station coupled with a Newport optical power-meter. All measurements were performed at room temperature (~25 °C), in ambient atmosphere.

Results and discussion

Electrochemistry of Ru-LC films

Cyclic voltammetry and potential steps

The cyclic voltammetry of the Ru-LC films show two, clearly defined chemically reversible waves (Fig. 1) with peak potentials at about 1.27 V (for the oxidation to the 3+ species) and −0.97 V (for reduction to the 1+ species) (potentials measured at scan rates ≤ 25 mV/s), with the anodic peaks always larger and sharper than the cathodic ones. These potentials are close to those found in aqueous solutions for dissolved $Ru(bpy)_3^{2+}$. At low scan rates, < 100 mV/s, the peak currents were proportional to the scan rate, v, as expected for a thin-film process. At larger scan rates a gradual shift towards a $v^{1/2}$ dependence was observed, which indicates the onset of a slow diffusional process within the film. The peak potentials did not depend on the scan rate for low scan rates (< 100 mV/s), where the currents were small and the ohmic drop through the film was negligible. In this region, the peak potential separations were about 80 mV for the oxidation scan and 120 mV for the reduction scan and the proportionality to scan rate essentially indicates total reduction or oxidation of the thin-film. The oxidation peak always showed a small pre-peak or shoulder (depending on the scan rate) in the forward scan when the positive scan followed a negative scan (Fig. 2); if the film was cycled only in the positive direction, no pre-peak was observed. The charge passed in the forward scan (Q_a) was always larger than the charge corresponding to the reverse scan (Q_c) (Table 1); for the anodic branch the difference was only about 10–15%. However, for similar experiments with an initial cathodic scan (not shown) the value could reach 30% or more. The charge was calculated after the background current was subtracted; for the cathodic branch this subtraction was more uncertain.

Double potential step experiments (between 0 and 1.3 V or 0 and −1.0 V) showed that only about 50% of the charge was recovered in the reverse step for 10 s steps (see Table 2). This difference between the charges passed on the forward step, Q_f, to 1.3 V (or −1.0 V) and the reverse step, Q_r, to 0 V is too large to be explained by irreversible electronic charge trapping in the film alone. If this much charge was trapped during one step, then a second double-step experiment would yield only very low currents during oxidation (or reduction), since most of the film would have already been oxidized (or reduced), and this was not the case. The double potential step experiments were reproducible and the charge

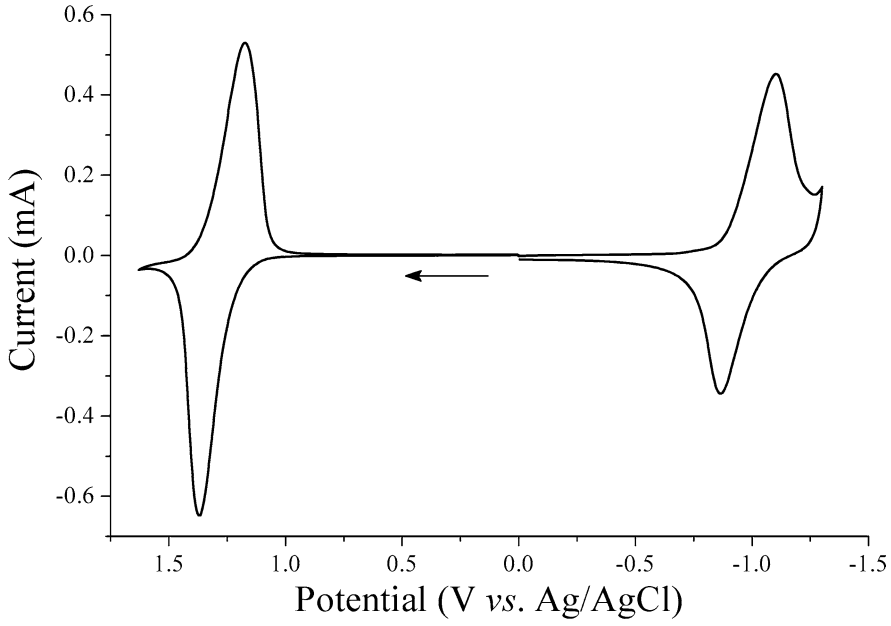

Fig. 1 Cyclic voltammetry of a spin-coated Ru-LC film (~150 nm thick) on ITO. Scan rate: 100 mV/s; $A \sim 1$ cm^2; solution: aqueous 0.1 M $KClO_4$

during oxidation (or reduction) did not change (within $\pm 5\%$) from one set of experiments to another.

The difference in the charge passed during the steps can be explained if one takes into account that the capacitive currents that pass during the first and second steps are different. Charge trapping in the film probably results in a different film capacity, leading to different charging currents. Some charge trapping process is still likely to occur after the film is oxidized (or reduced), charge which is removed only very slowly from the film, but it is difficult to estimate its value.

Ion transport through the film

As previously described, the peak currents depend linearly on the scan rate for low scan rates, but the dependence gradually changes to a $v^{1/2}$ one as the scan rate increases. This feature is consistent with a slow diffusional process, as described by Matsuda and co-workers for thin-film voltammetry [6].

These authors give an approximate analytical expression (accurate to within 0.5%) for calculating the peak current:

$$\frac{i_p}{nF} = 0.446 \frac{C^* D}{d} w^{1/2} \tanh\left(0.56 w^{1/2} + 0.05 w\right) \quad (1)$$

$$w = \frac{nF}{RT} v \frac{d^2}{D} \quad (2)$$

where C^* is the concentration of active sites in the film, D is the apparent diffusion coefficient (corresponding to the slowest mobile species: electrons, holes or counter-

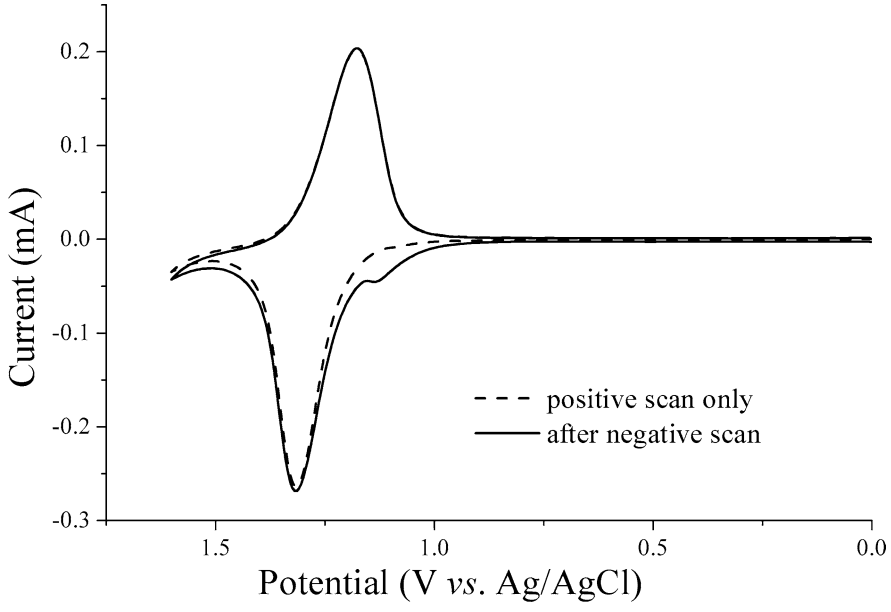

Fig. 2 Cyclic voltammetry of oxidation scans of a spin-coated Ru-LC film (~150 nm) on ITO. Scan rate: 100 mV/s; $A \sim 1$ cm^2; solution: aqueous 0.1 M $KClO_4$

Table 1 Dependence of anodic peak charge on scan rate

Scan rate (V/s)	Q_a(C), $\times 10^4$	Q_c(C), $\times 10^4$	Q_c/Q_a
0.005	6.7	2.5	0.38[a]
0.01	5.94	3.2	0.54[a]
0.025	6.1	4.4	0.72[a]
0.05	6.7	5.5	0.82
0.075	6.9	6.1	0.88
0.1	7.0	6.3	0.90
0.2	7.2	6.7	0.92
0.3	7.3	6.8	0.93
0.4	6.9	6.2	0.89

[a] Large background current; large errors after subtraction

Table 2 Typical charges in double potential step experiments

	Q_f1st step (C)	Q_r2nd step (C)	Ratio
0 V (10 s) to 1.3 V (10 s)	3.2×10^{-4}	1.8×10^{-4}	0.56
0 V (10 s) to −1.0 V (10 s)	4.0×10^{-4}	1.7×10^{-4}	0.43

ions) within the film, and d is the film thickness; all other parameters have the usual significance.

Figure 3 shows the scan rate dependence of the anodic peak current (forward scan) and the corresponding fit. For a 150 nm thick film, a two-parameter curve fitting gives values of about 4–6$\times10^{-10}$ cm^2/s for the apparent diffusion coefficient and 0.4–0.5 M for the concentration of active sites (neglecting the presence of pinholes and considering the total geometric area as the active film area). Films prepared with different added amounts of poly(methyl-methacrylate) showed similar values for the diffusion coefficient.

The corresponding values for the cathodic process were more difficult to obtain since a rather large background current was usually present (see Fig. 1). If the uncorrected peak currents are used to extract the same parameters, values of about 10^{-9} cm^2/s for the diffusion coefficient and 0.3 M for the active site concentration were obtained. The anodic process parameters did not change when $TMAClO_4$ was used as supporting electrolyte, while the cathodic ones showed a slightly smaller apparent diffusion coefficient ($\sim0.4\times10^{-9}$ cm^2/s). This trend suggests that during oxidation only ClO_4^- ions penetrate the film, as opposed to reduction, where some cations from the electrolyte may also move into the film to compensate for ClO_4^- that is not removed. This results in a smaller apparent diffusion coefficient when the bulkier $TMAClO_4$ is used as supporting electrolyte.

Film morphology

To check the film coverage of the ITO, experiments were carried out with ferrocene-methanol (FcMeOH), which oxidizes in a region where no film electrochemistry is observed, dissolved in the supporting electrolyte. Figure 4 shows the CV of FcMeOH on film-covered and bare ITO electrodes. The large value of the FcMeOH peak indicates an appreciable number of pinholes in the film. The FcMeOH CVs appear to be almost irreversible on the film-covered electrode at slow scan rates, but become more reversible at faster ones (Fig. 4, right). This is characteristic of the behavior of an electrode with an array of ultramicroelectrodes (in this case the pinholes) that are spaced sufficiently far apart that they are acting fairly independently [7].

AFM pictures of the film (Fig. 5, top) show a large number of pinholes in the film, proving that the film is rather porous and could act quite similar to an array of ultramicroelectrodes when a redox couple is present in solution.

Several attempts to seal the pinholes using ITO silanization or 2-aminophenol polymerization failed. In

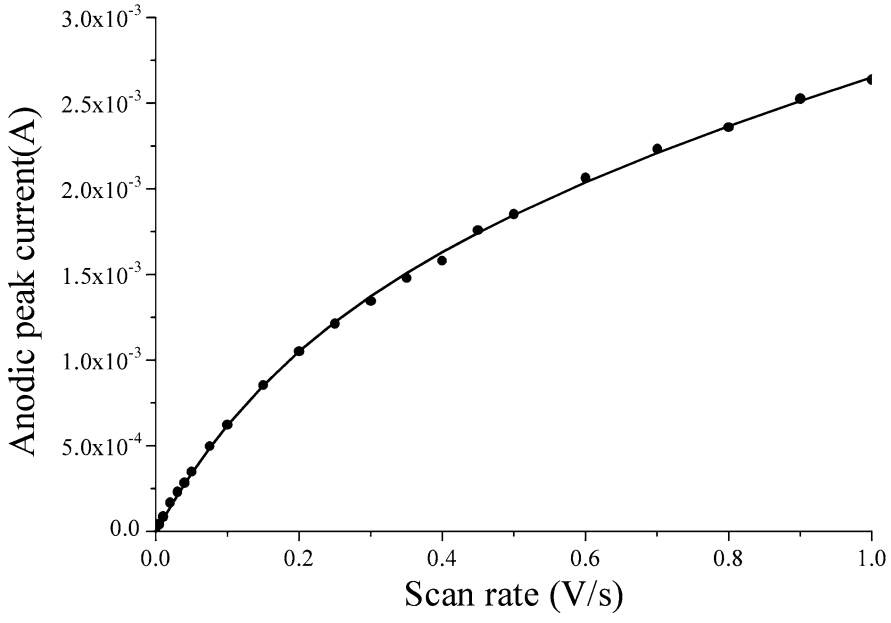

Fig. 3 Scan rate dependence of the anodic peak current (the line represents the fit with Eq. 1); 150 nm film thickness; $A\sim1$ cm^2; solution: aqueous 0.1 M $KClO_4$

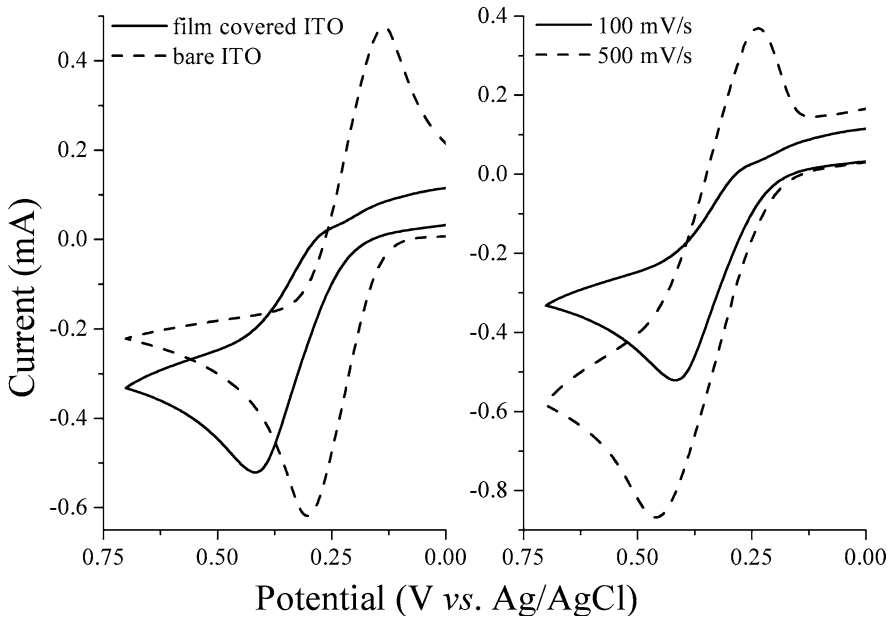

Fig. 4 Left: ferrocene-methanol cyclic voltammogram (CV) (~5 mM) on film-covered ITO and bare ITO; scan rate: 100 mV/s. Right: ferrocene-methanol CV (~5 mM) on film-covered ITO for two scan rates. 150 nm film thickness; $A \sim 1$ cm^2; solution: aqueous 0.1 M $KClO_4$

the case of ITO silanization, the silane derivative increased the surface pH, which resulted in the hydrolysis of the esterified ligand in the film and the film dissolving in water. In case of 2-aminophenol polymerization, during the polymerization process the Ru-LC film itself became covered with polymer, leading to much lower currents after electropolymerization. Apparently, a strong interaction between the polymer and Ru-LC allows the polymer film to grow outside the pinholes, even though the electropolymerization occurs at potential values at which the $[Ru(bpy)_2(bpy\text{-}LC)](ClO_4)_2$ film should be electronically resistive.

ECL of Ru-LC films

Potential scans

During a cyclic voltammetry scan, relatively strong ECL was observed during both oxidation and reduction (Fig. 6). The ECL results, as in solution phase ECL of $Ru(bpy)_3^{2+}$, from reaction of the +3 and +1 species. In this case, for an initial anodic scan, the +3 species is produced at the electrode and diffuses away (probably by charge hopping) in the film from the electrode surface. Upon a cathodic scan, any +3 charge remaining reacts with +1 species generated at the electrode to produce ECL. The ECL signal was stronger in the anodic branch, but the relative intensity of the ECL signal in the full-scan cyclic voltammetry experiments depends on the direction of the very first scan. If the scans are taken following a procedure to ensure similar conditions, such as one positive scan after two negative scans, or one negative scan after two positive ones, the relative height of the ECL signal is about the same (Fig. 7, 0 minutes wait). The ECL can still be observed even after long waiting times (up to 30 min) at zero volts with the cell on (Fig. 7). The behavior suggests charge trapping in the film: during the reverse scan, the films do not reach the initial +2 state, but some Ru^{3+} (or Ru^{+}) remains in the film and is slowly removed at zero volts (probably due to the high resistance of the film under these conditions). As a result, ECL can be seen when the film is scanned in the reverse direction due to the residual oxidized (or reduced) species still present.

Potential steps

When the potential of the $[Ru(bpy)_2(bpy\text{-}LC)](ClO_4)_2$ film was stepped between 1.3 V and −1.0 V, strong ECL was observed (Fig. 8). In this experiment the potential was stepped to one potential for the indicated time and then stepped to the other potential.

The data from double potential-step experiments show that the integrated ECL did not change for pulse durations longer than 3 s (Table 3), suggesting that after 3 s the film was fully oxidized (reduced). The charge, however, increased steadily as the pulse duration increased, but this may be due to the pinholes and corresponding background current. Ideally, after completely oxidizing (or reducing) the film in the first step, the charge passed in the second step should be exactly twice the charge passed in the first step (neglecting capacitive currents).

The data in Table 3 show rather large deviations, either smaller (for positive steps first), or larger (for negative steps first). This is not surprising though, since the charge passed during reduction was always smaller (compare column 2 in Table 3 and all the CVs – the cathodic currents are *always* smaller). The total (integrated) ECL emission was smaller if the film was first

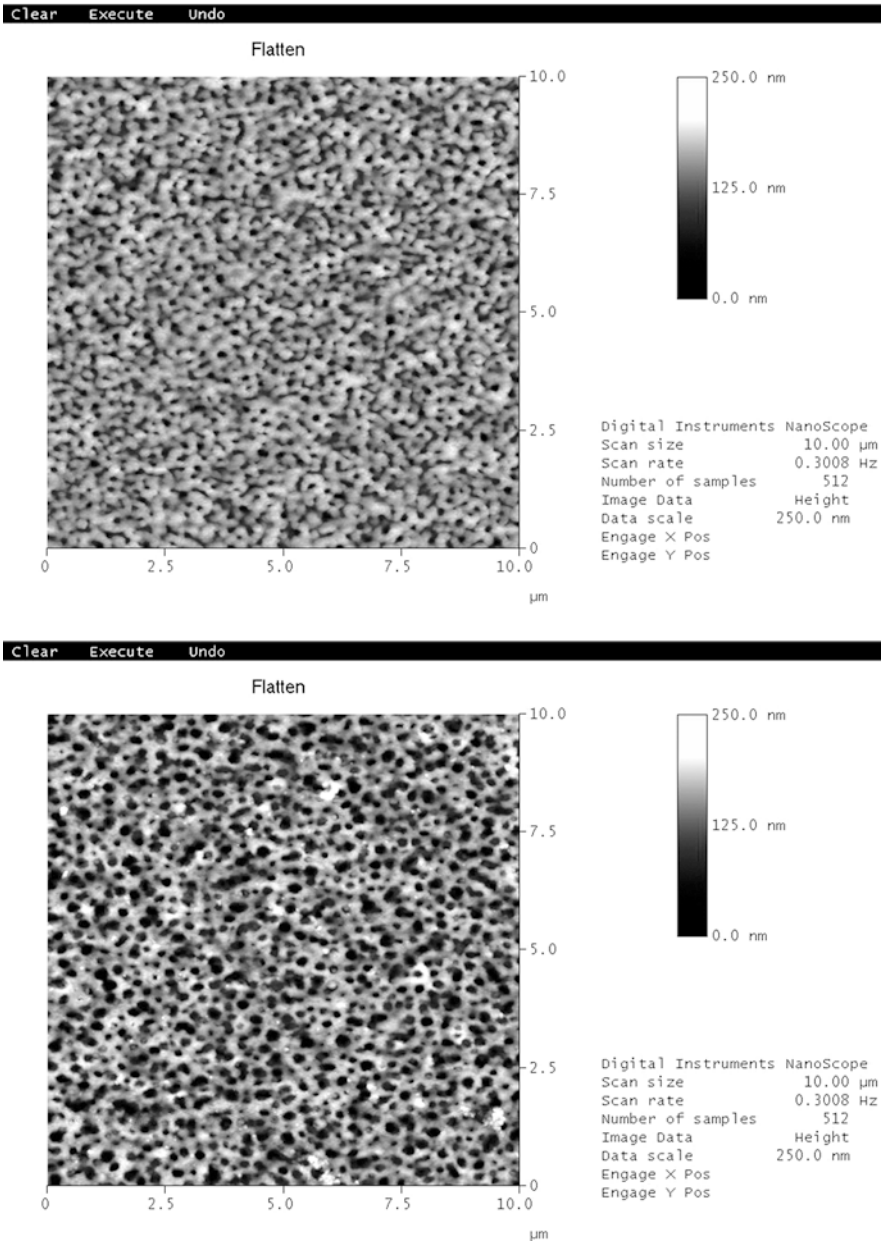

Fig. 5 AFM pictures of the pristine film (top) and after 50 oxidation/reduction cycles (bottom)

oxidized, probably because the oxidized species is a better quencher than the reduced species.

Degradation of the Ru-LC films

The electrochemistry of the Ru-LC films changed as the film was scanned continuously in the electrolyte solution (Fig. 9). Both the anodic and cathodic peaks decreased, while two small peaks that appeared to be chemically reversible developed at 0.63 and 0.85 V. At the same time, the ECL signal decreased dramatically during continuous cycling.

Since Ru-LC is an ester and previous studies [8] found that they hydrolyze in water even at only slightly alkaline pH (8.2), we have tested the film electrochemistry at pH 5, 3 and 1 by adding $HClO_4$ to the electrolyte. No improved stability was found at pH 5, but instead, as the pH became more acidic (≤ 3) the ITO dissolved through the pinholes and a dissolution peak appeared at approximately −0.65 V. At pH 1 the dissolution was so fast that the reduction peak of the film was no longer visible and the entire film simply delaminated along with ITO dissolution after two or three scans. The results suggest that the film degradation is not related to its hydrolysis in the water-based electrolyte.

The substrate on which the film is spin-coated did not have any effect on the film stability upon cycling and similar results were obtained when the film was spin-coated onto HOPG and glassy carbon, both of which are more stable during reduction than ITO (Fig. 10).

This behavior suggests that the degradation is an intrinsic property of the film and is not related to sub-

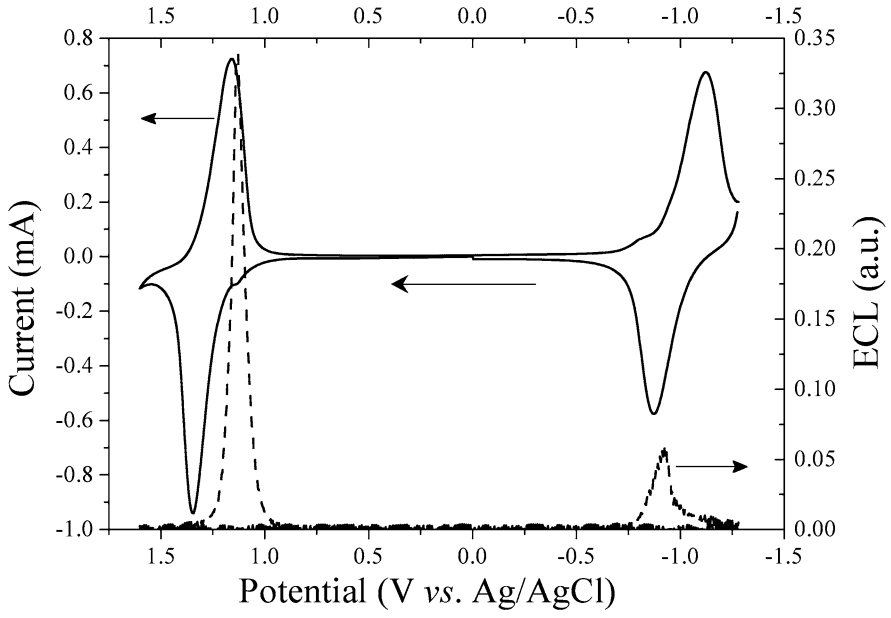

Fig. 6 CV and ECL for a Ru-LC film (~150 nm) spin-coated onto ITO. Scan rate: 200 mV/s; A~1 cm^2; solution: aqueous 0.1 M $KClO_4$

strate dissolution and film delamination. The film does not appear to dissolve in the electrolyte during continuous cycling: the absorption spectra of the electrolyte after scanning the film for 100 cycles did not show any peaks that could be related to dissolved film material.

The absorption spectrum of the film changed, however, during cycling. Fig. 11 left shows the absorption

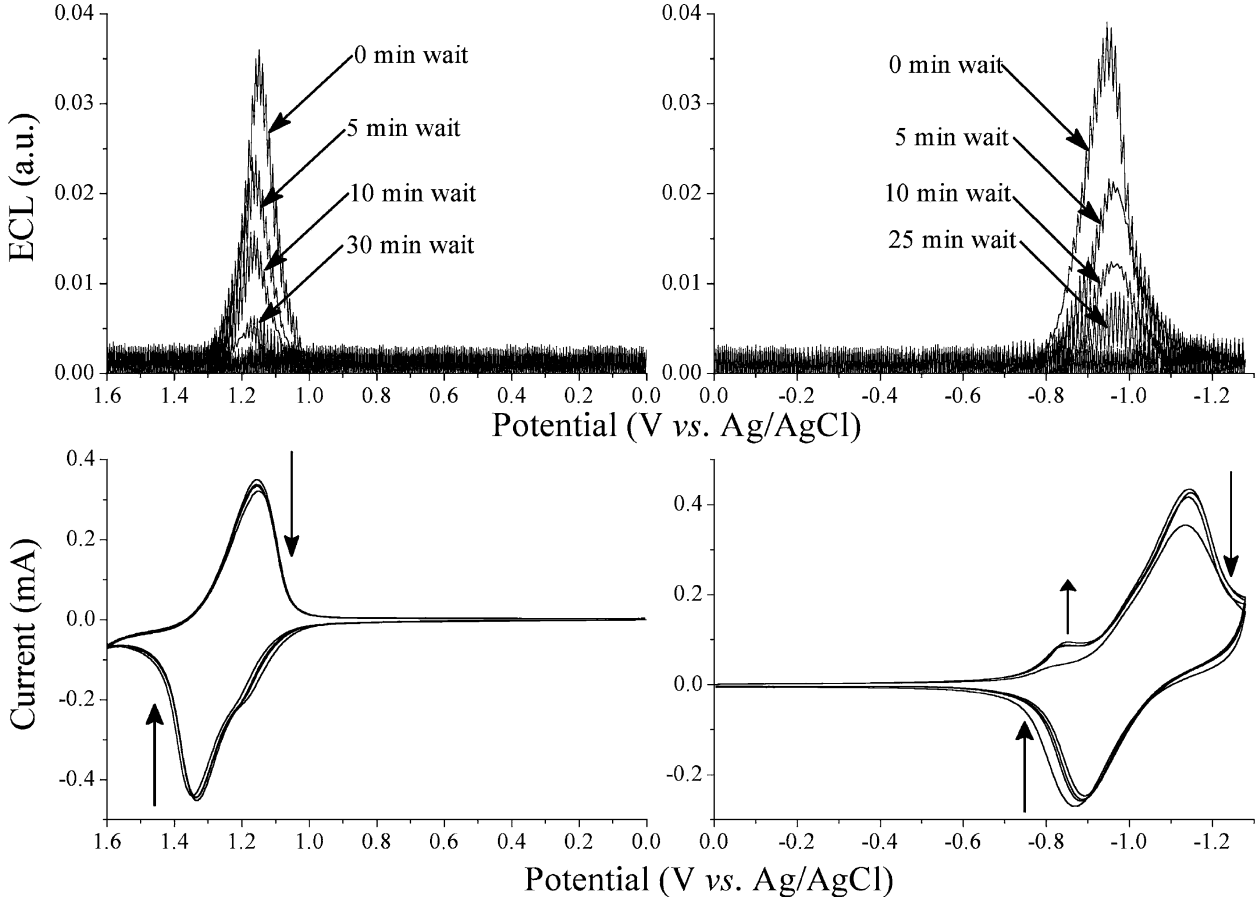

Fig. 7 ECL and CV for a Ru-LC film (~150 nm) spin-coated onto ITO as a function of waiting time at 0 V (cell on). Left: one positive scan following (after waiting at 0 V) two negative scans. Right: one negative scan following (after waiting at 0 V) two positive scans. Scan rate: 200 mV/s; A~1 cm^2; H_2O + 0.1 M $KClO_4$ (the small cathodic peak that appears at long waiting times corresponds to O_2 reduction)

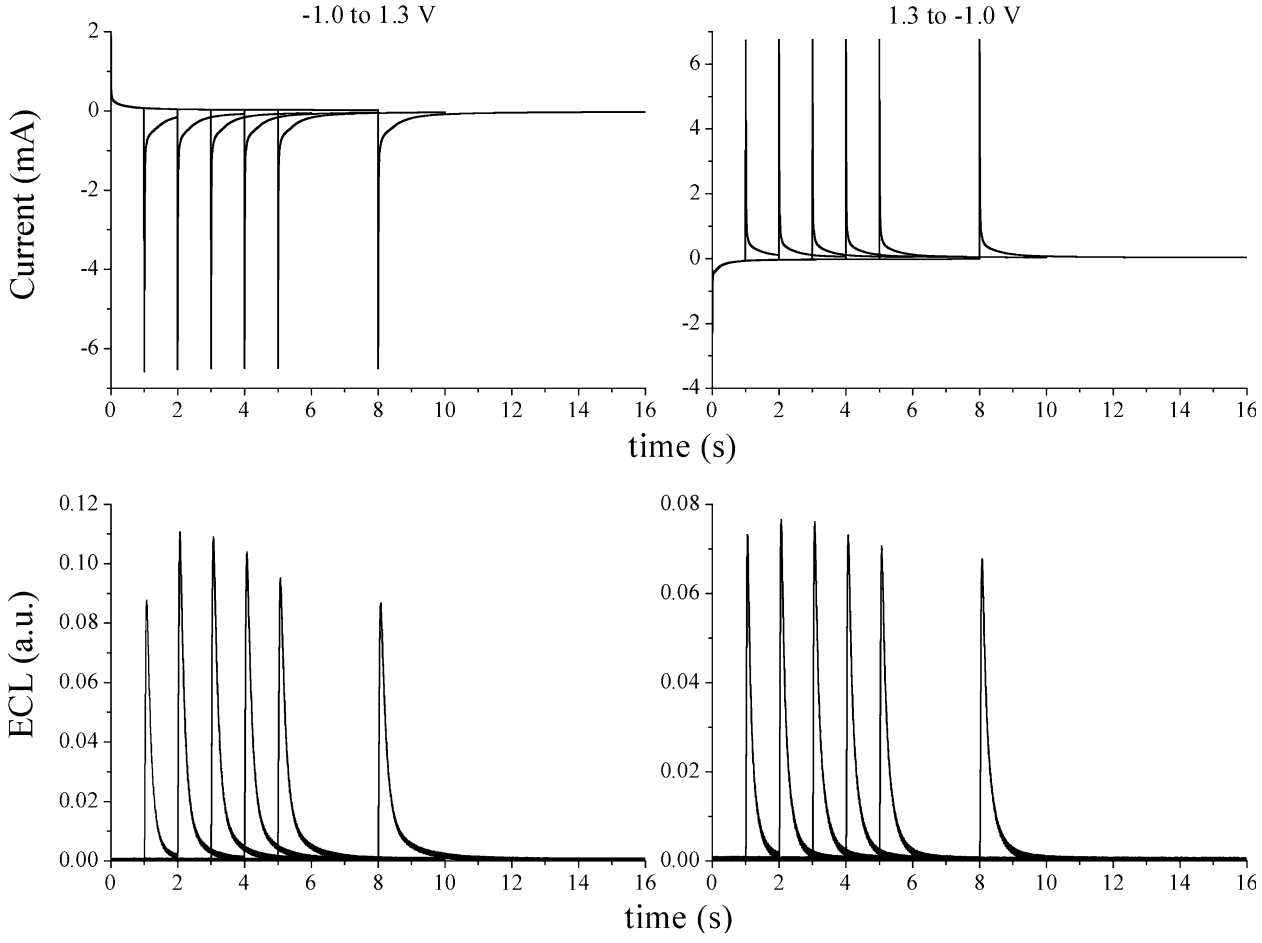

Fig. 8 Top: current and ECL for potential steps between −1.0 V and 1.3 V. Bottom: current and ECL for potential steps between 1.3 V and −1.0 V. Step durations are 1, 2, 3, 4, 5 and 8 s at each potential

spectrum of the pristine film and after 50 cycles. The spectrum of the pristine film is similar to the spectrum obtained in solution (Fig. 11, right), but the spectrum after 50 cycles at 100 mV/s is quite different: the peaks become less resolved, and the total absorption increased compared to the pristine film. The change can be easily observed visually, since the film changed color from orange-yellow to pale-brown.

If the film was scanned for 50 cycles only in the positive direction (Fig. 12, left), no apparent change was seen in the electrochemical behavior and the film appeared to be much more stable. On the other hand, if the film was scanned only in the negative direction, the film changed its electrochemical behavior quite rapidly (Fig. 12, right); after 50 cycles the reduction peaks almost disappeared into the background current and the oxidation peaks became much smaller. This suggests that the reduced species is much less stable than the oxidized one, as already known for other tris(bipyridine) Ru(II) derivatives [9]. The film morphology also changed during continuous cycling (Fig. 5): the pinhole area increased as the film was cycled and the film became more porous. The cyclic ion insertion/de-insertion processes, as well as solvent penetration are probably responsible for such morphological changes in the film.

Finally, the electrochemistry degraded to some extent when the film was simply left in the electrolyte for long durations (10–12 h). The film presumably slowly hydrolyzes leading to changes in both its composition and morphology.

Solid-state devices

Since related polymeric derivatives have already been used as emitters in light-emitting electrochemical cells, showing fairly good performance [10, 11], we tested two-electrode solid-state devices prepared by Ga-In printing on top of the Ru-LC films, similar to $Ru(bpy)_3$ ones [1, 3]; the most important features are outlined below (Fig. 13).

First, the current flowing through these devices is about three orders of magnitude smaller than $Ru(bpy)_3$ devices. The small current (and consequently, low brightness) is a result of very small electron and hole mobilities through the film. Even when folded, the long alkyl chains will considerably increase the separation between the ruthenium sites and, therefore, electron-hopping between Ru-centers is seriously hindered. Moreover, the very hydrophobic nature of the film

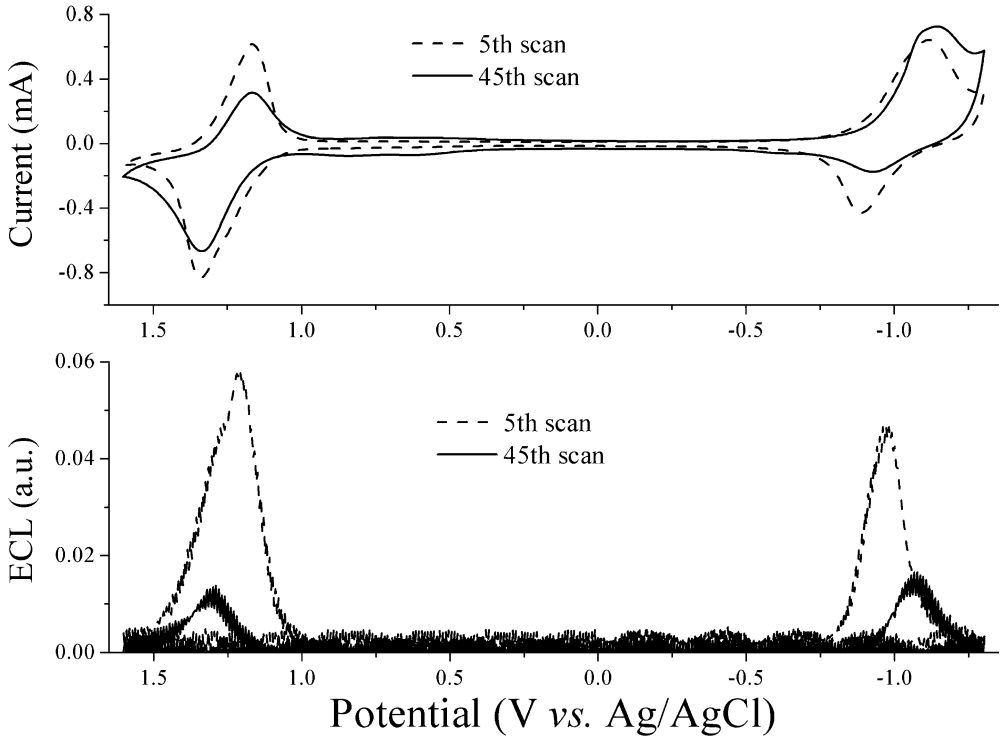

Fig. 9 Effect of continuous cycling of the Ru-LC film on ITO. Scan rate: 200 mV/s; $A \sim 1$ cm^2

Table 3 Charge and integrated ECL in double potential-step experiments

Step duration (s)	Positive step first				Negative step first			
	1.3 V step charge, $\times 10^4$ (C)	−1.0 V step charge, $\times 10^4$ (C)	Integrated ECL (a.u.)	Charge ratio	−1.0 V step charge, $\times 10^4$ (C)	1.3 V step charge, $\times 10^4$ (C)	Integrated ECL (a.u.)	Charge ratio
1	2.01	3.38	0.144	1.69	1.52	4.82	0.185	3.17
2	2.48	4.22	0.174	1.71	2.02	5.87	0.274	2.91
3	2.85	4.80	0.187	1.69	2.31	6.61	0.302	2.86
4	3.17	5.31	0.192	1.68	2.54	7.18	0.303	2.83
5	3.49	5.82	0.191	1.67	2.75	7.79	0.299	2.84
8	4.18	7.03	0.194	1.68	3.35	9.26	0.303	2.76

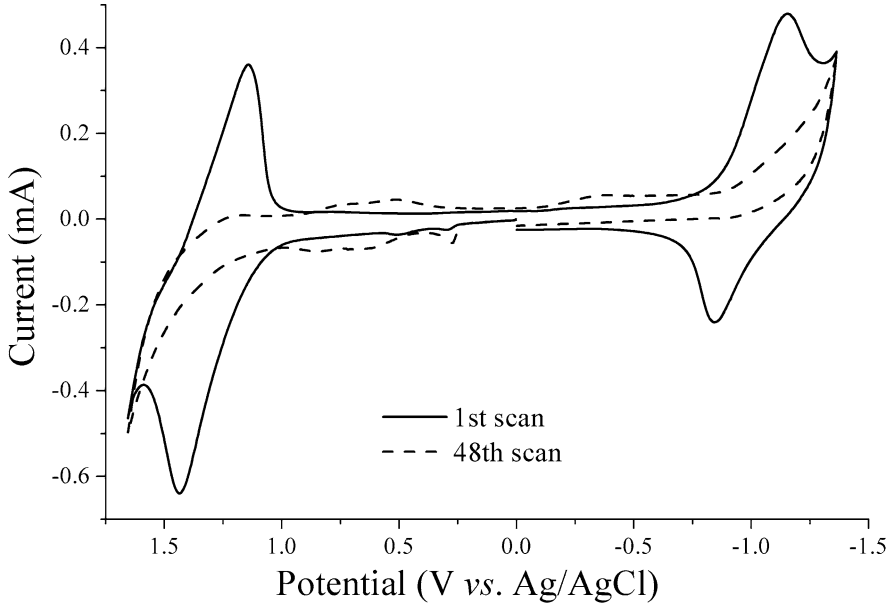

Fig. 10 Effect of continuous cycling of the Ru-LC film on HOPG. Scan rate: 100 mV/s; $A \sim 1$ cm^2

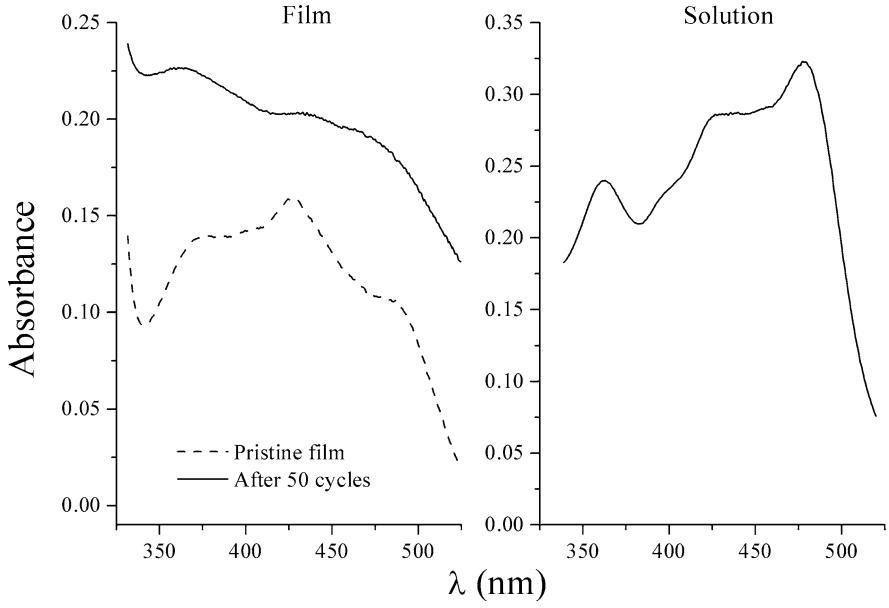

Fig. 11 Absorption spectra of: the pristine film (left, dashed line); the film after 50 oxidation/reduction cycles (solid line, left); Ru-LC in acetonitrile, 25 μM (right)

hinders the uptake of the small amounts of water that might be important in anion mobility and device performance [12]. Second, the maximum quantum efficiency of these devices is about one order of magnitude lower than the other $Ru(bpy)_3$ devices (Fig. 13).

Although both the total current and quantum efficiency are much smaller, the current and luminescence transients are quite similar to the $Ru(bpy)_3$ devices, showing a rather sharp luminescence decay, but little to no change in current (Fig. 14).

Fig. 12 Continuous cycling of the Ru-LC film during oxidation (left) and reduction (right). Scan rate: 100 mV/s, $A \sim 1$ cm^2. The insets show the evolution of the peaks during the cycling

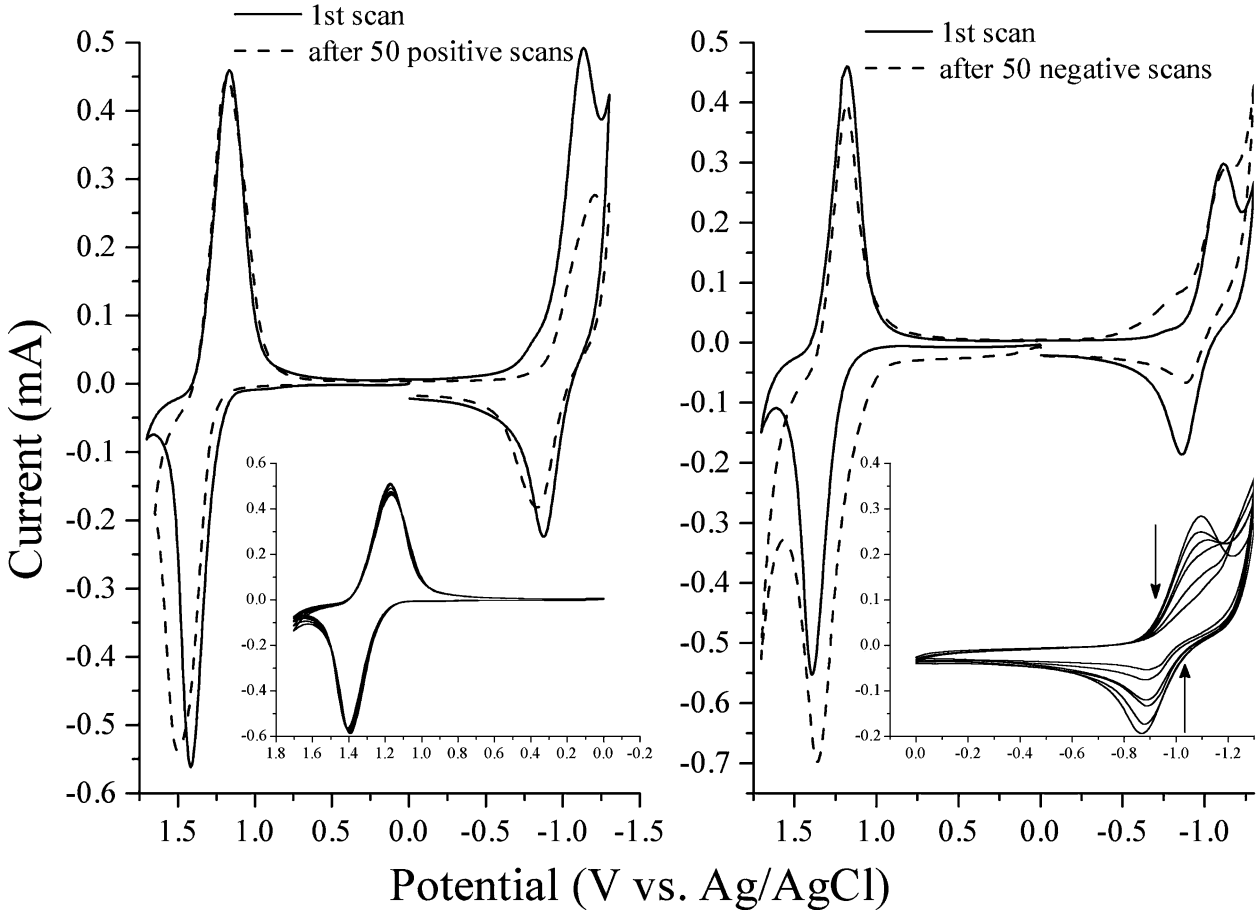

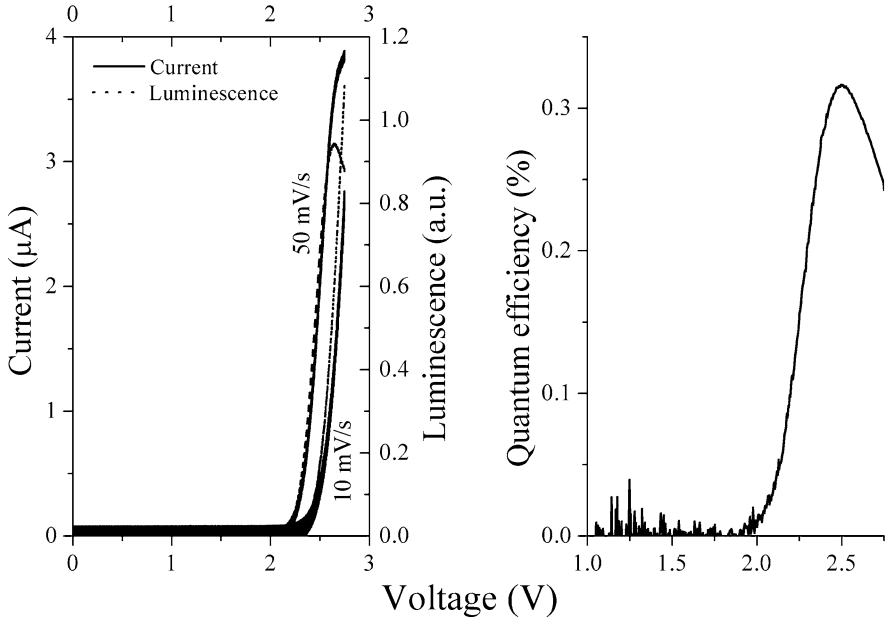

Fig. 13 Current-voltage and luminescence-voltage characteristics for a Ru-LC film (150 nm, GaIn)

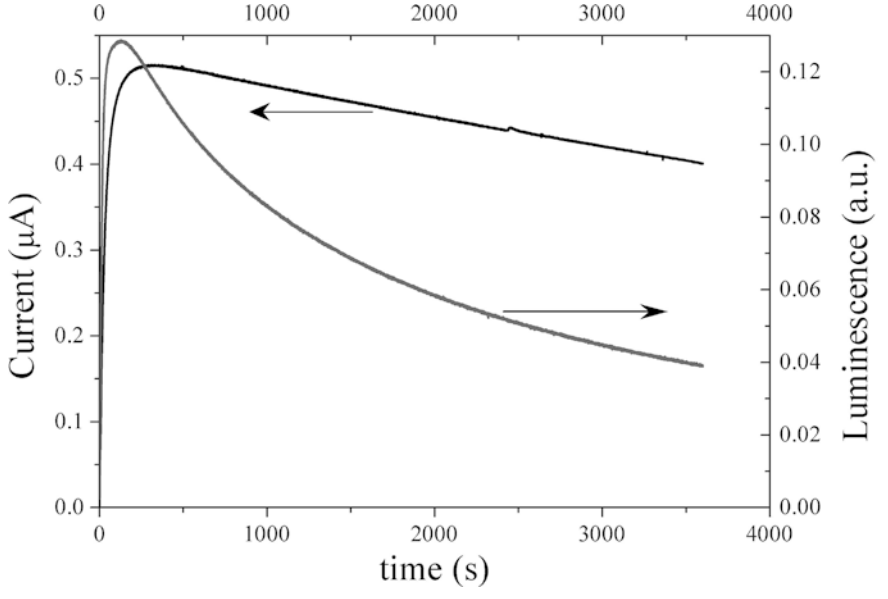

Fig. 14 Current and luminescence transients at 2.25 V applied voltage for a Ru-LC film (150 nm, GaIn)

Conclusions

Thin solid film electrochemistry and ECL of Ru-LC was studied in aqueous solution. The film exhibits reversible electrochemistry both in oxidation and reduction. The apparent diffusion coefficient of perchlorate ions in the film was found to be $\sim 5\times10^{-10}$ cm^2/s.

Thin solid films of Ru-LC exhibit strong ECL when scanned between −1.25 and 1.65 V or when the potential is stepped between 1.3 V and −1.0 V. Both the electrochemistry and ECL degrade rather quickly as the potential is continuously scanned or stepped; the film's degradation appears to be related to the instability of the reduced state.

The film has a rather porous structure, with many small pinholes. Their number and size increases as the film is continuously cycled in solution; ion insertion/deinsertion probably plays an important part in increasing the film's porosity.

Two-electrode solid film luminescence devices show a behavior similar to $Ru(bpy)_3^{2+}$ devices, but the current is three orders of magnitude smaller (probably because of the large separation between the Ru^{2+} sites) and the hydrophobicity of the films, while the quantum efficiency is about one order of magnitude lower.

Acknowledgements Support for this research from the National Science Foundation (CHE 0202136) and the U.S. Army Research Office MURI (DAAD-19–01–1-0676) is gratefully acknowledged.

References

1. Buda M, Kalyuzhny G, Bard AJ (2002) J Am Chem Soc 124:6090
2. Rudmann H, Shimada S, Rubner MF (2002) J Am Chem Soc 124:4918
3. Gao FG, Bard AJ (2002) Chem Mater 14:3465
4. Buda M (2004) Devices/polymers. In: Bard AJ (ed) Electrogenerated chemiluminescence. Marcel Dekker, New York
5. Sprintschnik G, Sprintschnik HW, Kirsch PP, Whitten DG (1977) J Am Chem Soc 99:4947
6. Aoki K, Tokuda K, Matsuda H (1983) J Electroanal Chem 146:417
7. Bard AJ, Faulkner LR (2001) Electrochemical methods. Wiley, New York, pp 619–623
8. Gaines GL Jr, Behnken PE, Valenty SJ (1978) J Am Chem Soc 100:6549
9. Tokel-Takvoryan NE, Hemingway RE, Bard AJ (1973) J Am Chem Soc 95:6582
10. Lee J-K, Yoo D, Rubner MF (1997) Chem Mater 9:1710
11. Wu A, Yoo D, Lee J-K, Rubner MF (1999) J Am Chem Soc 121:4883
12. Pile D, Bard AJ (2004) unpublished experiments